Investigation of Cascadia Tremor Correlation with Earth Tides

Carl W. Ulberg
Senior Integrative Exercise
March 9, 2007

Submitted in partial fulfillment of the requirements for a Bachelor of Arts degree from Carleton College, Northfield, Minnesota

Table of Contents

Investigation of Cascadia Tremor Correlation with Earth Tides

Carl W. Ulberg
Carleton College
Senior Integrative Exercise
March 9, 2007

Advisors:
Kenneth C. Creager, University of Washington
Sarah J. Titus, Carleton College

ABSTRACT

Major episodes of episodic tremor and slip located along the Cascadia subduction zone occur every ~14 months and have been well-studied using both seismic and geodetic data. I look at the interval between major events using vertical component data from 11 Pacific Northwest Seismograph Network seismometers broadly distributed across western Washington and find that there are still tremor episodes, although of smaller duration and magnitude. Typical smaller tremor bursts occur over 2 to 3 days, containing periods of up to 8 continuous hours exhibiting similar waveforms, and appear in 2 to 8 stations at a time. I compare the occurrence of tremor episodes with Coulomb stresses due to Earth tides and ocean tidal loading, and find a possible correlation between the two data sets.

Keywords: Earth tides, Cascadia subduction zone, earthquakes, seismology, correlations

INTRODUCTION

Cascadia subduction zone non-volcanic tremor is a recently discovered phenomenon (Dragert et al., 2001). It can be identified by unique non-earthquake seismic signals associated with slow slip events along the deeper portion of the subduction interface (Dragert et al., 2001; Rogers and Dragert, 2003). Tremor has also been observed in the Nankai subduction zone in Japan and along the San Andreas fault of California (Obara, 2002; Johnston, 2006). The exact mechanism behind tremor is unknown, but one possibility is the movement of fluid in the subduction zone due to the dehydration of the subducting slab (Obara, 2002). Tremor has been associated with changes in plate motion as measured using GPS data. It is important to study tremor because it is believed that it can add to stress in the locked portion of a plate boundary interface, thereby increasing the chance of a large, damaging earthquake (Rogers and Dragert, 2003).

The first evidence for tremor in the Cascadia subduction zone was found in Washington State and Vancouver Island, Canada, in 2001 (Dragert et al., 2001). Since then, it has been determined by Dragert et al. (2001) and others that major tremor bursts occur along the Cascadia subduction zone every ~14 months. Each burst lasts for approximately two weeks, during which the tremor occurs almost continuously over a broad 50-100 km area. GPS data compared with these tremor bursts show that there is slip in the movement of the North American plate associated with tremor (Rogers and Dragert, 2003; Dragert et al., 2001). This process is known as episodic tremor and slip.

In this study I examine tremor in the state of Washington for the year of 2006 using seismic data. During this year there were no large episodic tremor and slip events. However, there were smaller bursts of tremor, and I compare the occurrence of these tremor events with tidal cycles, for both ocean tides and Earth tides. Specifically, I seek to determine whether the stresses on the Earth due to ocean and earth tides are large enough to trigger a tremor episode, and if tremor occurs at times when the stresses are aligned correctly. This can help to better determine the mechanisms for causing tremor.

GEOLOGIC SETTING

Cascadia Subduction Zone

The Cascadia subduction zone results from the oblique subduction of the oceanic Juan de Fuca plate beneath the continental North American plate (Fig. 1). This subduction zone has been active since the Mesozoic, beginning with the Farallon plate subducting beneath North America (Wilson, 1998). At approximately 30 Ma, the Juan de Fuca plate separated from the rest of the Farallon plate along the Pioneer fracture zone, which is near the Mendocino fracture zone shown in Figure 1 (Wilson, 1988). Since 30 Ma, the convergent margin has been rotating clockwise due to being caught in the larger dextral shear boundary between the North American and Pacific plates (Wells et al., 2002).

For the last 20 Ma, convergence between the Juan de Fuca and North American plates has been relatively constant at a rate of ~40 mm/yr in a N55°W direction (Wilson, 2002). Currently, convergence rates change along strike from ~30 mm/yr at 42°N to ~45

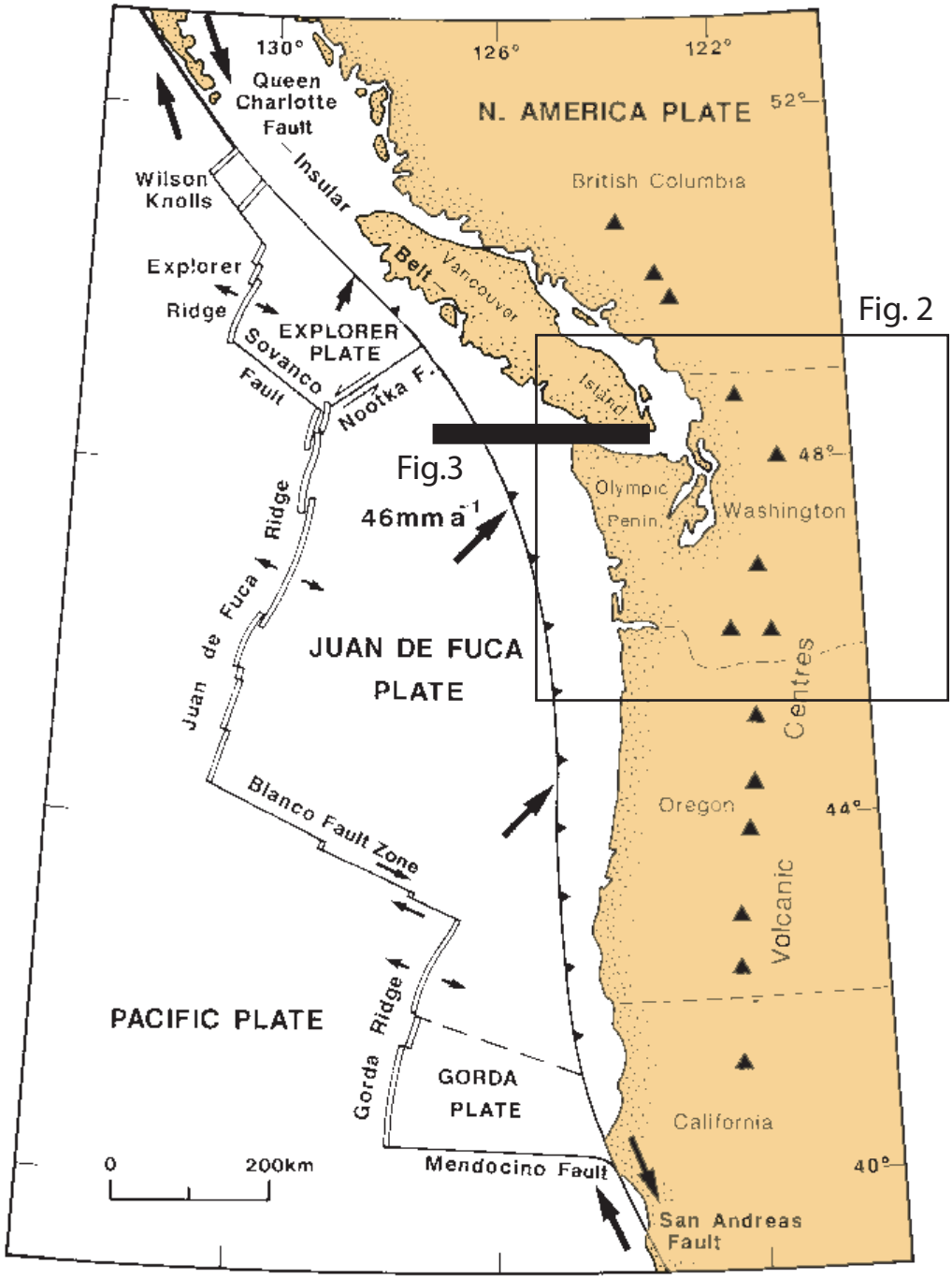

Figure 1. Tectonic context of the Cascadia subduction zone, from Dragert et al. (1994). The Cascadia subduction zone occurs where the oceanic Juan de Fuca plate subducts beneath the continental North American plate. Square box indicates Figure 2 map location and bold line indicates Figure 3 cross-section location.

mm/yr at 49°N, although these along-strike differences have changed through time (DeMets et al., 1990).

Subduction of the Juan de Fuca plate is relatively shallow compared to many subduction zones, with a dip angle of ~10° in the first 50 km of depth (Crosson and Owens 1987). There is an arch in the plate near the latitude of the Puget Sound, causing a bend of ~45° in the strike of the plate (see plate depth contours in Fig. 2). South of this bend the Juan de Fuca plate strikes almost due north, and north of this bend the plate strikes in a N45°W direction. This bend is attributed to a geometric space problem caused by the Juan de Fuca plate subducting into a concave oceanward corner of the North American plate. (Crosson and Owens, 1987; Trehu et al., 2002; Chiao and Creager, 2002)

The Cascadia subduction zone has ruptured periodically (every ~600 yrs) in giant megathrust earthquakes (M_w>8) throughout the Holocene (Atwater, 1987; Satake et al., 1996). These earthquakes are interpreted to occur on the locked portion of the interface between the Juan de Fuca and North American plates (Fig. 3). This zone is located at depths of ~10 km and temperatures of ~350°C, from 40 to 90 km off the coast of the western United States (Hyndman, 1997). The last major thrust earthquake occurred in 1700, and is believed to have ruptured the entire Cascadia convergent margin, resulting in a tsunami which reached as far away as Japan (Atwater, 1987; Satake et al., 1996).

Intraslab earthquakes occur within the subducting Juan de Fuca plate, and have a larger potential for causing damage in North America than offshore megathrust earthquakes (Preston et al., 2003). This is because they can occur directly underneath the continent and beneath major urban centers. For example a M_w=6.8 earthquake ruptured

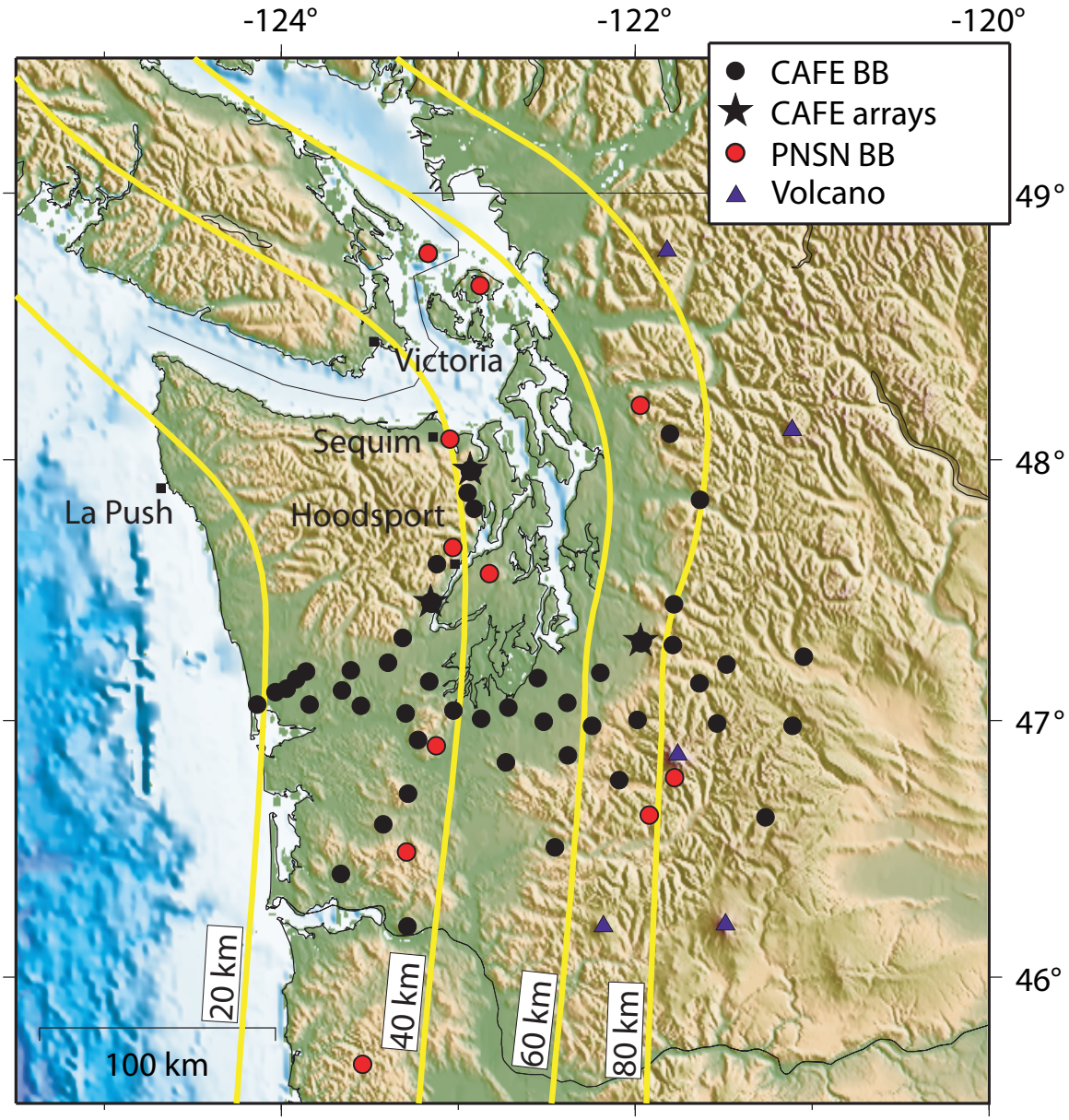

Figure 2. Map showing the CAFE deployment as well as the PNSN broadband stations used for this study. Depth contours (thick yellow lines) of the subducting Juan de Fuca plate are shown every 20 km. Modified from Abers et al. (2007).

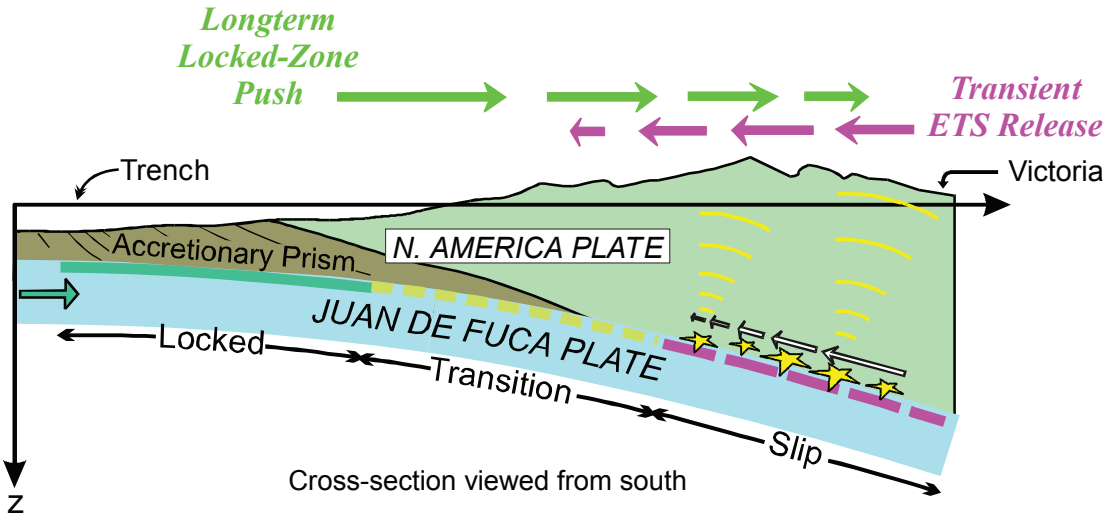

Figure 3. Cross-section of the Cascadia subduction zone near Vancouver Island, showing basic mechanisms of episodic tremor and slip. Approximate tremor locations are indicated by stars. From Geological Survey of Canada.

underneath Nisqually in the south Puget Sound in 2001, causing much property damage to the greater Puget Sound area, including Seattle (Preston et al., 2003).

Previous Work on Tremor in Cascadia

Tremor in Cascadia occurs primarily between 25 and 35 km in depth, although it can range from 11-48 km (Rogers and Dragert, 2003; Kao et al., 2005). Much of the tremor occurs near the interface between the Juan de Fuca plate and the North American plate, both within the subducted slab and in the overriding crust (Fig. 3; Kao et al., 2005). Locations of tremor are primarily under the Puget Sound and the southeast tip of Vancouver Island, above the 40 km depth contour of the Juan de Fuca plate (Rogers and Dragert, 2003; Kao et al., 2005), although they can also occur as far south as northern California (McCausland et al., 2005). Figure 3 shows the basic mechanisms of episodic tremor and slip in Cascadia.

The frequency content of tremor as a seismic signal is in the range between 1 and 6 Hz. This is lower than the frequency range found for small earthquakes, which is normally above 10 Hz (Rogers and Dragert, 2003; Kao et al., 2005). A tremor signal is usually emergent rather than impulsive (meaning that it increases gradually without any clear starting point), and can last anywhere from several minutes to several hours. Tremor signals are strongest on horizontal seismographs and are thought to move at shear wave velocities of ~4 km/s (Obara, 2002; Rogers and Dragert, 2003). In order to be classified as tremor, a tremor-like signal must be seen on multiple seismographs in a network, with each signal exhibiting a similar shape (Rogers and Dragert, 2003).

Otherwise, noise from wind or cultural sources at a particular seismogram could be mistaken for tremor.

The exact cause of tremor is unknown, but one possibility is the movement of fluid in the subduction zone, possibly related to the dehydration of the subducting slab (Obara, 2002; Kao et al., 2005). Dragert et al. (2001) and others have theorized that tremor episodes can add to the cumulative stress on the locked portion of the Juan de Fuca-North American plate interface, increasing the probability of a large, megathrust earthquake.

METHODS

Studying Tremor

Instrument Deployment

This project began as part of an IRIS internship at the University of Washington, supervised by Ken Creager. My involvement for the internship included helping to scout locations and deploy 62 broadband seismometers around the western part of the state of Washington during the summer of 2006 (Fig. 2). This deployment was for the CAFE (Cascadia Array For Earthscope) experiment, which is part of the Earthscope initiative.

Some of the requirements for selecting a site for a seismometer were: open sky (for solar panels), some distance (>1 km) from major roads and cities (to reduce noise and to lessen the risk of vandalism), and reasonable proximity to smaller roads (for transport of seismometer, batteries, cement, etc.). For these reasons, many of the

seismometers were placed in clearcuts owned by timber companies, although there were some on private or government property.

Examination of Seismic Data

For this study, I examined data from eleven seismometers broadly distributed across western Washington and northwest Oregon (Fig. 2). These seismometers are similar to the ones that were deployed for the CAFE experiment, but are maintained by the Pacific Northwest Seismograph Network. Data were collected for the year of 2006, although due to winter conditions, four different stations were used starting in November. I looked at the vertical component data from broadband or short-period instruments that were band-pass filtered at 1.5 to 5 Hz (The data were run through a Fourier transform, and the high- and low-frequency signals were discarded; the data were then run back through an inverse Fourier transform to enhance the seismic signal over periods of 0.2-0.7 s). An envelope function (envelope functions emphasize times when seismic energy is highest by essentially squaring the signal) calculated from the resulting waveforms was then low-pass filtered at 0.05 Hz (this enhances the signal over periods of 1/.05=20 seconds).

A tremor episode was classified as an emergent increase in seismic activity across multiple stations lasting from 10 minutes to several hours. Tremor must be observed with similar waveforms at different stations since a signal at a single station could likely be the result of noise from wind or cultural sources. For this study, observations were done by hand. Figure 4 shows an example of data from the eleven seismometers where

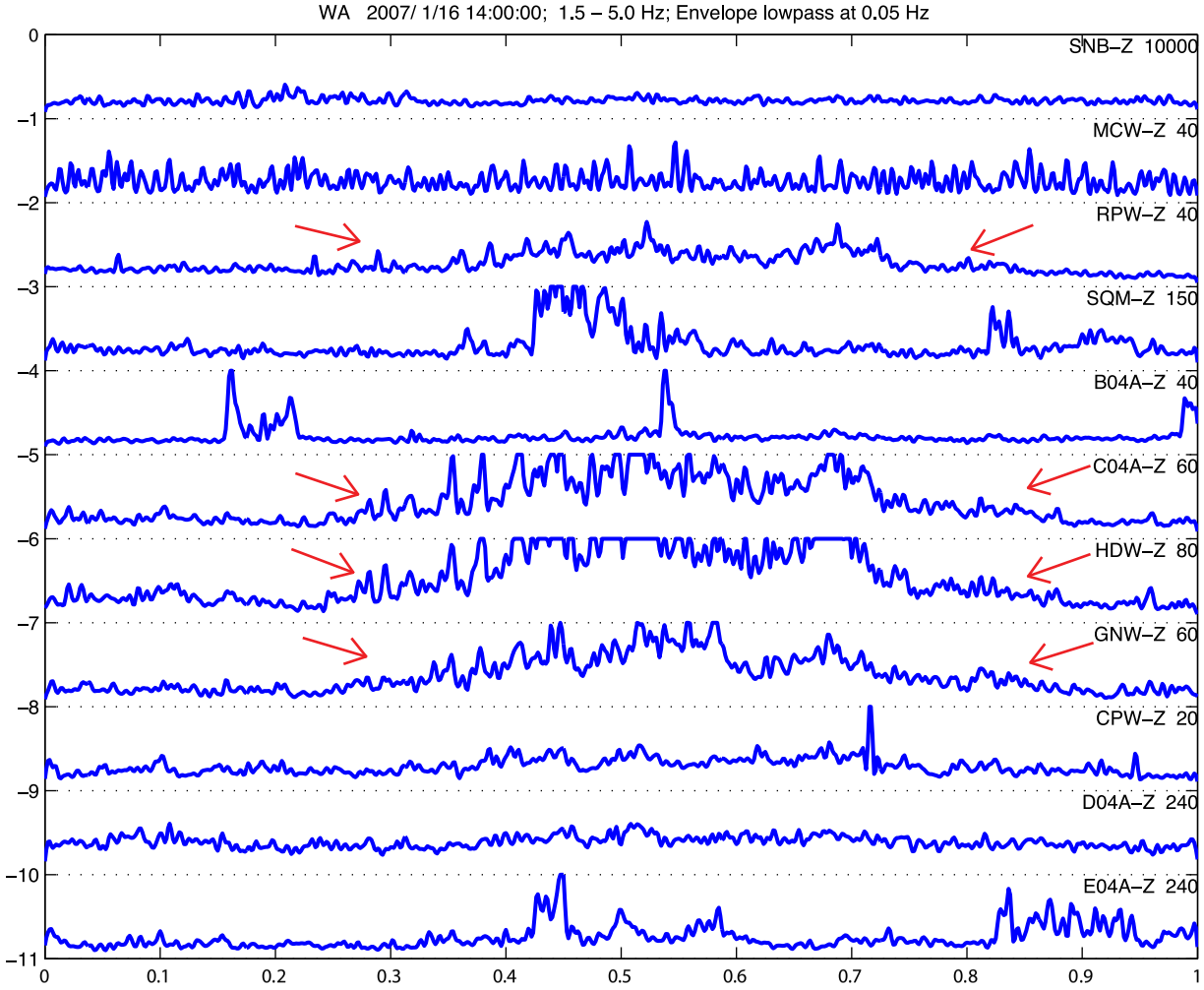

Figure 4. Example of a pdf file with envelope functions showing tremor in several stations. Horizontal axis is one hour, vertical axes are scaled differently for each station. In this example, stations 3, 6, 7, and 8 all exhibit a similar emergent waveform between .3 and .75 hours (shown with arrows), which is classified as tremor.

tremor was identified at 4 stations (stations 3, 6, 7, and 8). Note the similarity in the shapes of the waveforms.

Once a tremor episode was identified, the starting time (all times used in this study are reported as Greenwich Mean Time), duration, and stations in which it was present were recorded. At the end of the year, this data was combined into one time series containing the number of hours of tremor that occurred during each day of the year. Consecutive days exhibiting tremor were classified as single 'events.'

Examination of Possible Tremor Causes

Ocean Tides Data Set

Predicted ocean tide heights were downloaded for the tidal gauges at La Push, WA and Sequim, WA (Fig. 2), and from the NOAA (National Oceanic and Atmospheric Administration) website. These two locations give the tides along the Pacific coast of Washington as well as within the Strait of Juan de Fuca. Predicted ocean tides were also obtained using software from Agnew (1996), assuming the tidal model of Schwiderski (1980). This method yields similar results to the NOAA data.

In order to determine how the ocean tides changed over the course of the year, the tidal range (the difference between maximum and minimum tide) was computed for each day of 2006.

Earth Tides Data Set

Data to study Earth tides were obtained from software by Agnew (1996). This software calculates stresses at the surface of the Earth due to Earth tides as well as ocean

tidal loading, in the form of a stress tensor. Stress tensors are useful because they can be used to obtain a traction vector on a plane of interest (in this case, the plane approximating the Juan de Fuca plate under Washington state). Traction is defined as force per unit area (the same as stress), and can be decomposed into three components: (1) a component in the direction normal to the plane, (2) a component within the plane in question and in the direction of slip on the fault, and (3) a component within the plane in question and perpendicular to the previous two. Table 1 shows the vectors used to describe the Juan de Fuca plate. The two components of the traction vector that are used for this study are in the normal direction and in the slip direction. The magnitudes of these vectors are equal to the normal and shear stresses on the plane, respectively. See Appendix A for a detailed explanation of these calculations.

Table 1. Vectors describing the Juan de Fuca plate.

Vector	**Components**
Strike of plate (v_1)	<cos *a*, sin *a*, 0>
Dip of plate (v_2)	<-sin *a* cos *b*, cos *a* cos *b*, sin *b*>
Normal to plate (v_3)	<sin *a* sin *b*, -cos *a* sin *b*, cos *b*>
In direction of plate motion (v_{slip})	slip=<cos(*dir*) sin(*dir*) 0> -direction of plate motion at surface v_{slip}=slip-dot(slip,v_3)*v_3; -projection onto plane

With *a* as the strike angle and *b* as the dip angle of the subducting plate, and *dir* as the direction of slip (Fig. 5). In calculating v_{slip}, dot() signifies dot product. The coordinate system used is x=North, y=East, z=down

Stress tensors were obtained at 30-minute intervals at four points above the Juan de Fuca plate (Table 2). These sites were chosen because of their positions above the subducting plate with different strikes, as determined from a depth contour plot similar to Figure 2. Three points are on land near the projection of the 40 km slab depth contour, the primary zone of tremor occurrence, and one point (La Push) is off the coast of Washington to provide a reference point for ocean tidal loading.

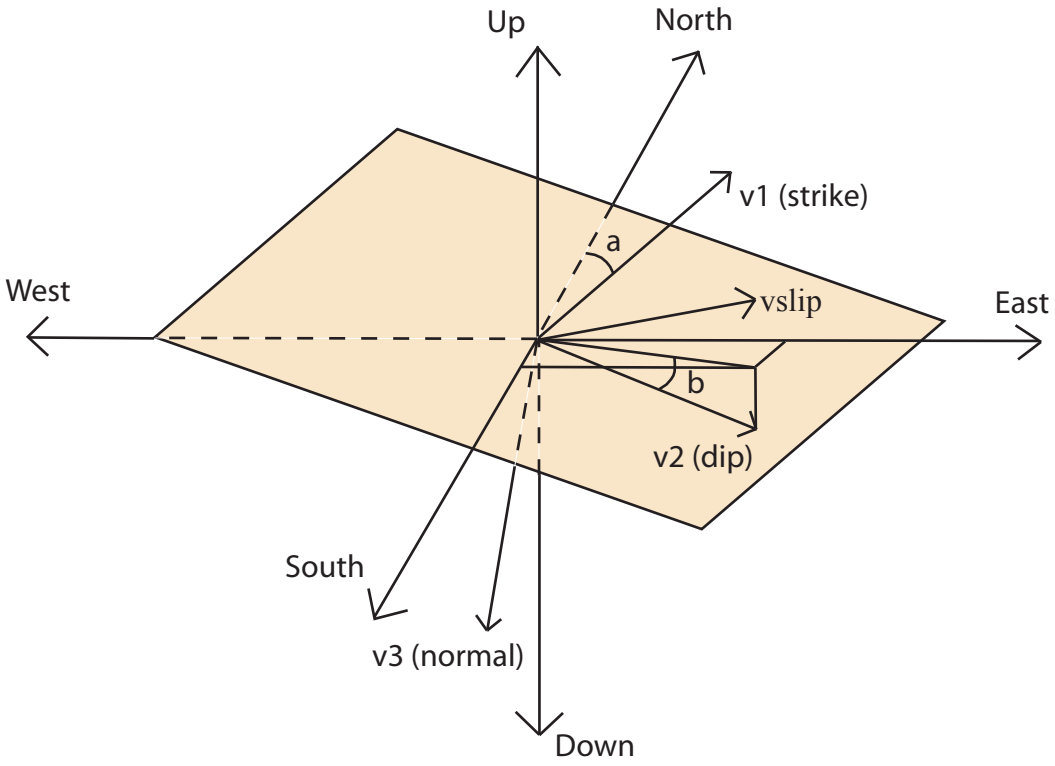

Figure 5. Geometry of a plane representing the Juan de Fuca plate. The plane can be described by three vectors: v1 (in the direction of strike), v2 (in the dip direction), and v3 (normal to the plane). The vector in the direction of slip (vslip) is within the plane. A point on the Juan de Fuca plate where it strikes approximately N15E as in this figure would be found in southern Washington.

Table 2. Sites for tensor calculations (see Fig. 2 for map locations)

Site	Latitude (°N)	Longitude (°W)	Approximate Strike of Juan de Fuca Plate (°)	Approximate Depth of Juan de Fuca plate (km)
La Push, WA	47.90	124.65	315	15
Victoria, BC	48.44	123.39	315	40
Sequim, WA	48.04	123.13	345	40
Hoodsport, WA	47.51	123.08	0	40

In order to quantify the change in shear and normal stresses at these points, a Coulomb stress analysis was used, as described by Cocco and Rice (2002). Shear and normal stresses can be used to determine Coulomb stress changes on a given fault using the following relation: failure due to frictional faulting occurs when the shear stress exceeds the coefficient of friction multiplied by the effective normal stress, or

$$\sigma_s \geq \mu(-\sigma_n - p), \tag{1}$$

where σ_s is shear stress (in the direction of slip), σ_n is normal stress (positive for extension), μ is the coefficient of friction of the rocks (typically between 0.6 and 0.8; Harris, 1998), and p is pore pressure. Although pore pressure has a large effect on Coulomb stress calculations, it is ignored in this study by assuming that it does not change. Additionally, a value for μ of 0.6 was used for this study.

This relation (1) can be better quantified by the Coulomb stress, $\sigma_s + \mu\sigma_n$. Large values for the Coulomb stress correspond to the largest probability of fracture along the Cascadia subduction interface. It is important to note that the stresses on the Juan de Fuca fault are modulated by many factors besides Earth tides, but this study focuses on the change in Coulomb stress due to tides. To calculate a stress time series to compare to tremor events, the maximum tidal Coulomb stress was calculated for each day of 2006.

Comparison of Earth Tides and Ocean Tides

Before comparing ocean and Earth tides with tremor, it is important to understand how these two data sets relate to each other. To do this, I plotted the ocean and Earth tides together on daily and monthly scales. Figures 6 and 7 show the ocean tide height plotted for one day with shear, normal, and Coulomb stress on the Juan de Fuca plate at two points used for this study, La Push and Sequim. The stresses at La Push were calculated several miles off the coast at the bottom of the ocean, whereas the stresses at Sequim were calculated several miles inland at the surface. This was done to examine the effect of ocean tidal loading on the data sets.

The plots appear somewhat similar due to diurnal or semi-diurnal tides, with two peaks and two troughs a day, with one peak possibly more pronounced. However, there are several obvious differences, which can be attributed to the effect of ocean tidal loading. First, the amplitude of the shear and normal stresses at La Push are orders of magnitude larger than the stresses at Sequim, due to the fluctuations in tidal height (a 1 m displacement of water equates to $1.00*10^3$ kg/m^3*9.8 m/s^2*1 m ≈ 10 kPa). Second, peaks (or troughs) in stresses at Sequim are shifted by 1-2 hours in relation to the ocean tide, whereas the stresses and ocean tide at La Push line up almost exactly. This is again due to the large effect of ocean tidal loading at La Push. Third, the sign of the normal stress switches between Sequim and La Push- at La Push, the shear and normal stresses have the same sign, whereas at Sequim the shear and normal stresses have opposite signs. The sign of the normal stress at La Push can be explained by high ocean tide corresponding to the maximum compression on the Earth from ocean tidal loading. Because extensional stress is positive in this stress data set, this would explain the negative (compressive)

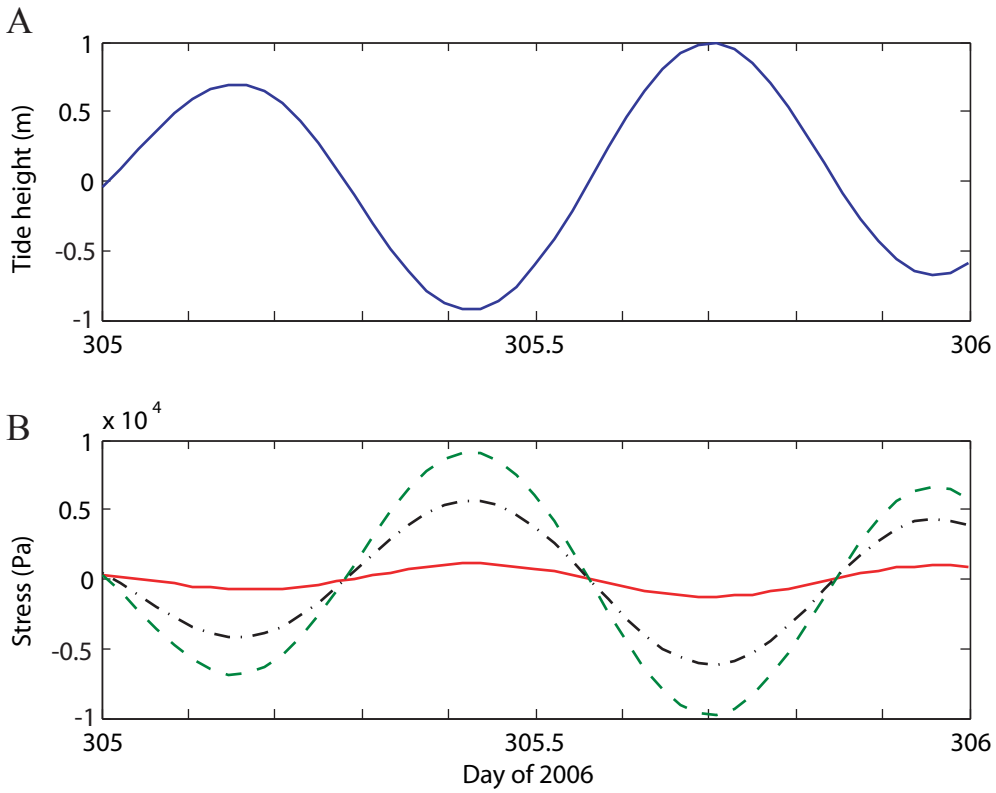

Figure 6. Comparison of ocean tide with stresses due to Earth tides and ocean tidal loading at La Push, WA for November 1, 2006. (A) Ocean tidal height. (B) Calculated shear (solid red), normal (dashed green), and Coulomb stress (dot-dashed black) on the Juan de Fuca plate.

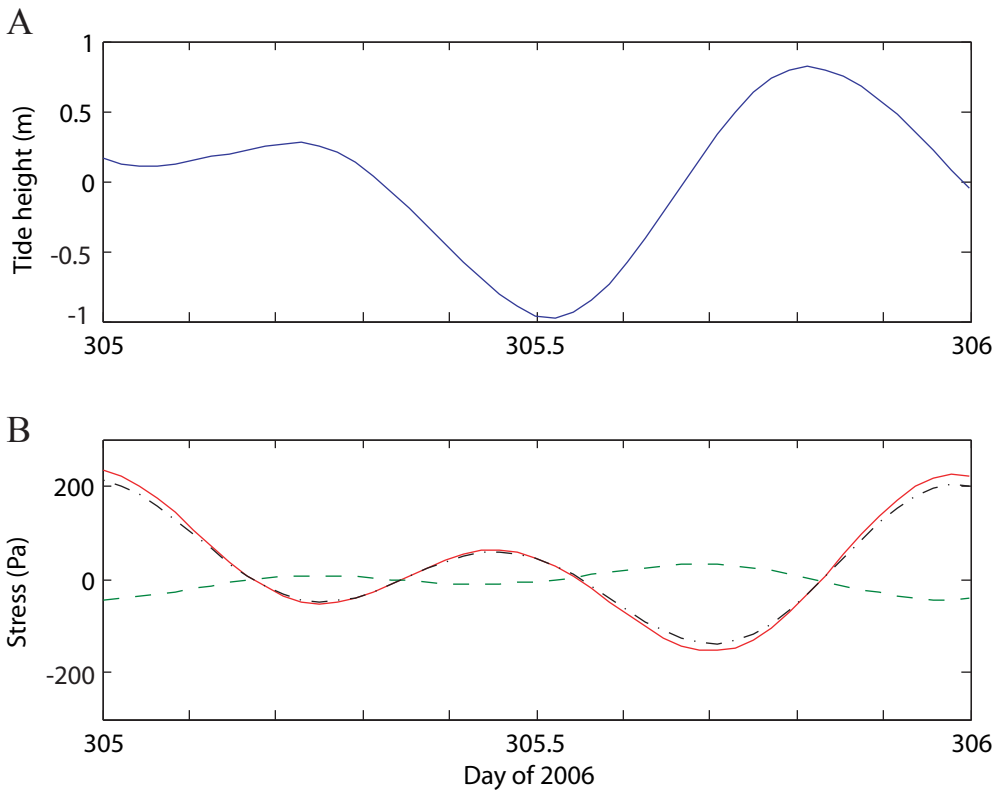

Figure 7. Comparison of ocean tide with stresses due to Earth tides and ocean tidal loading at Sequim, WA for November 1, 2006. (A) Ocean tidal height. (B) Calculated shear (solid red), normal (dashed green), and Coulomb stress (dot-dashed black) on the Juan de Fuca plate.

normal stresses during high tide. If the Sequim tensor were calculated at a point with fluctuating levels of water above it, it would have a similar behavior, and conversely, if the tensor calculated at La Push were at a point on land, it would resemble the results from Sequim. Indeed, when a tensor was calculated at the surface at La Push, it exhibited similar characteristics to the Sequim stresses.

Figures 8 and 9 show the ocean tide height plotted with shear, normal, and Coulomb stress for the month of November, at La Push and Sequim. Shear and normal stresses vary on a spring/neap cycle at the same times as ocean tides. Spring tide, when these values have the largest range, occurs when the moon and Sun are in alignment with the Earth (during new and full moons, also known as syzygy). Additionally, neap tide, when these values have the smallest range, occurs when the moon and Sun are out of alignment with the Earth (during the first and third quarter of the moon, also known as quadrature).

Based on examination of Figures 6-9, maximum Coulomb stresses occur near low ocean tides, when the sum of the shear and normal (extensional) stresses on the Juan de Fuca plate interface is at a maximum. These stresses are greater under the ocean, but still exhibit the same qualitative characteristics on land, due to the low value for normal stress. Furthermore, maximum Coulomb stresses will be greatest during spring tides, when there are the lowest low tides. These results are supported by Wilcock (2001), who found that earthquakes occur more frequently along the Juan de Fuca Ridge near low tides, and especially the lowest spring tides, attributed to maximum extensional stresses in all directions.

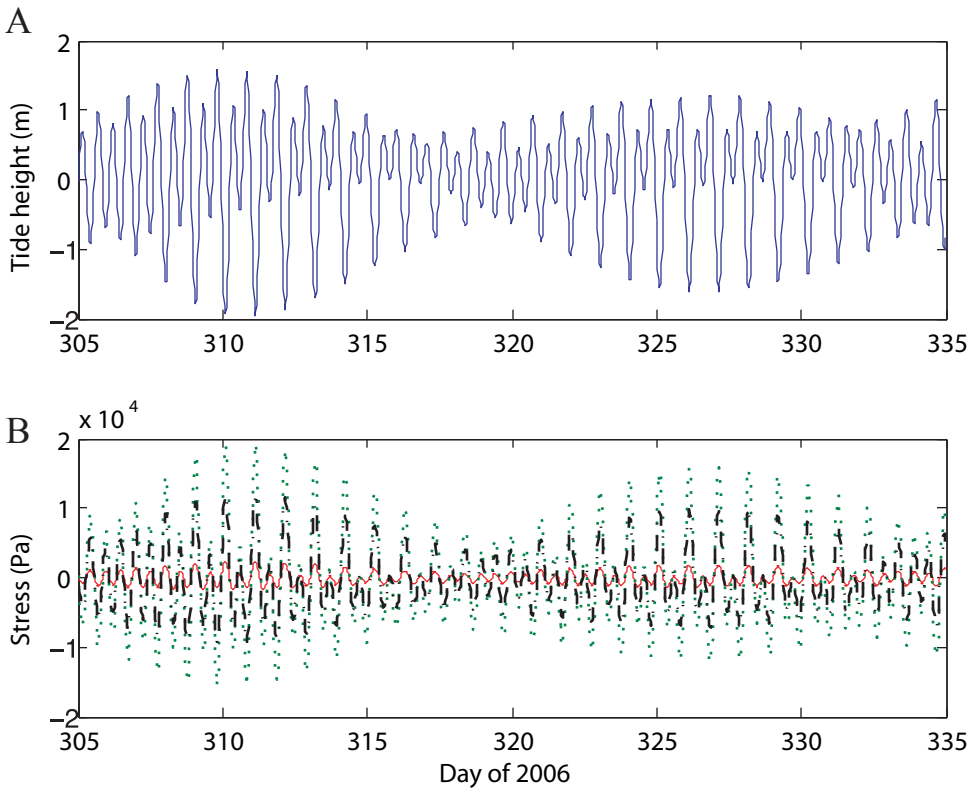

Figure 8. Comparison of ocean tide with stresses due to Earth tides and ocean tidal loading at La Push, WA for the month of November, 2006. (A) Ocean tidal height. (B) Calculated shear (solid red), normal (dashed green), and Coulomb stress (dot-dashed black) on the Juan de Fuca plate.

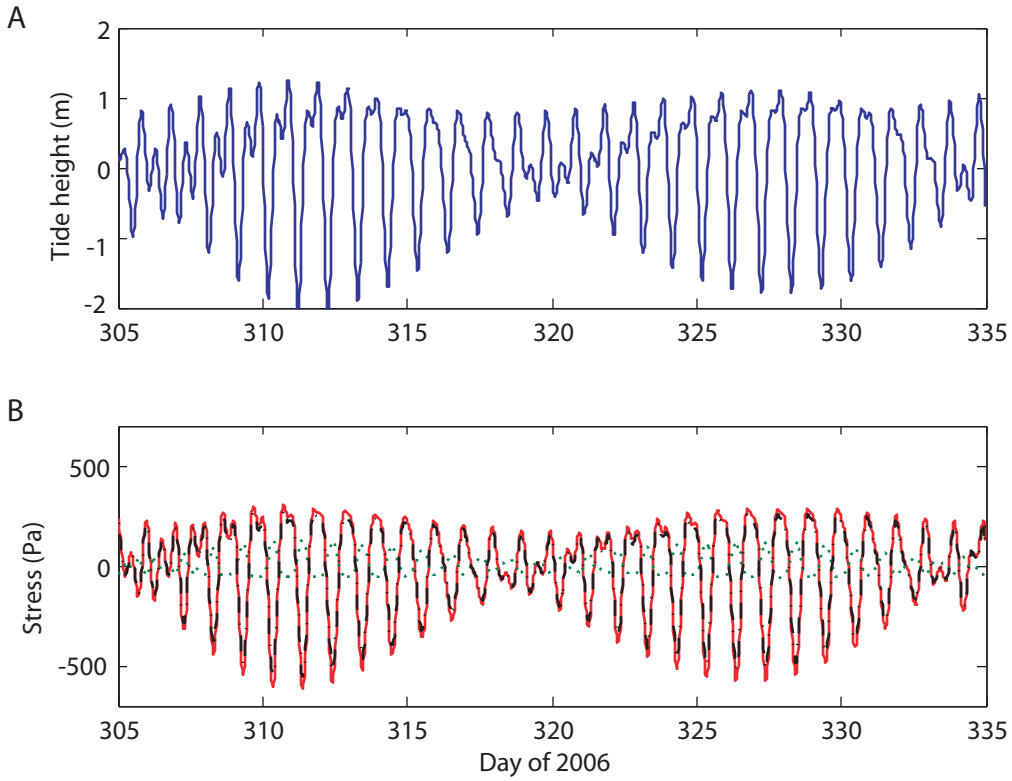

Figure 9. Comparison of ocean tide with stresses due to Earth tides and ocean tidal loading at Sequim, WA for the month of November, 2006. (A) Ocean tidal height. (B) Calculated shear (solid red), normal (dashed green), and Coulomb stress (dot-dashed black) on the Juan de Fuca plate.

Comparison of Earth Tides and Ocean Tides with Tremor

In order to compare tremor with earth and ocean tides, I used the following hypothesis: tremor occurs as slip along the interface between the Juan de Fuca and North American plates, and this slip is most likely to occur when the Coulomb stress due to Earth tides in that orientation is at its greatest. On a daily scale, the Coulomb stress due to Earth tides is greatest during low ocean tide, so this hypothesis would predict more tremor occurring during low ocean tides on a daily scale. On a monthly scale, Coulomb stresses due to Earth tides are greatest during spring tide (that is, the lowest low tides and their associated large Coulomb stresses occur during spring tide), so the hypothesis predicts more tremor occurring during spring tide on a monthly scale. For this study, I focused on the monthly scale, using two methods to determine a correlation between spring tide and tremor occurrences. To perform correlation tests between tides and tremor, I used Matlab version 7.3.0.267 (R2006b). See Appendix C for the code.

For the first test, cross-correlations were performed between tremor and ocean tidal range (as calculated at La Push and Sequim, WA), as well as between tremor and maximum Coulomb stress (as calculated at La Push, Sequim, Victoria, BC, and Hoodsport). This method gives a measure of the similarity between two data sets. The output is a third time series with length 2N + 1, where N is the length of the two original series (in this case, N=365 days). Each point on the new series represents the correlation at a certain lag between the two original series when they have been shifted that many days with respect to each other. A time series cross-correlated with itself would give a maximum correlation value at a lag of 0 days. In this analysis, a peak correlation at 0 lag

would indicate that tremor is well-correlated with either maximum ocean tidal range and/or maximum Coulomb stress.

The second test for correlation between tremor and tides is similar to that described by McNutt and Heaton (1981). This test divides the year into bins representing days before or after peaks (local maxima) in the tidal time series (in either ocean tidal range or maximum Coulomb stress). Each day of the year was assigned to a bin depending on how far removed it was from the closest tidal maximum. Then the number of hours of tremor and days with tremor were determined for each bin. Since maxima in ocean tidal range or Coulomb stresses did not occur at regular intervals, the bins near the edge (at +/- 8 days) have fewer possible days or hours with tremor.

RESULTS

Tremor

Tremor during the year 2006 can be characterized as a series of small tremor events (relative to the large 14-month episodic tremor and slip events), each usually lasting two to three days and typically containing 5-10 hours of tremor a day, with extremes of 0.5-18 hours in one day. A total of 259.5 hours of tremor occurred during 77 days of 2006, and these were divided into 38 tremor events, ranging from 0.5 hours in one day to 61 hours over five days (see Appendix B for a listing of tremor events). The number of stations that recorded tremor ranged from two to eight for each tremor episode. There was usually a period of one to two weeks between these tremor episodes,

although a period of 20 days without tremor was recorded in October. Figure 10 shows tremor events for 2006.

Comparison of Tremor with the Tides

A preliminary comparison of tremor with ocean tidal range and maximum Coulomb stress is shown in Figure 11, in which the time series are simply plotted together. There is no obvious correlation between the data sets, although it appears that many tremor bursts occurred at or near times of peak tidal range and maximum Coulomb stresses. Of course, there were also tremor episodes that occurred during low tidal ranges or low variations in maximum Coulomb stresses.

Cross-correlations of tremor with ocean tidal range (Fig. 12) and maximum Coulomb stress (Fig. 13) generally show a peak near 0 lag. This indicates that the data sets are best correlated when shifted by <2 days, which means that peaks of tremor generally occur at the same times as peaks in ocean tidal range and maximum Coulomb stresses. The peaks are repeated at intervals of approximately 14 and 28 days because of the inherent cyclicity of the tides. This repetition of peaks means that in order to read these figures, one must focus on the interval between shifts of –14 and +14 days. In Figure 13A, there is a clearer peak near 0 lag for the cross-correlation between maximum Coulomb stress and tremor at the La Push site as compared to the three other sites. In fact, the cross-correlation at Victoria has a dominant peak at –6 days away from 0 lag (Fig. 13B), and the cross-correlation at Sequim has a peak at +1 lag that is lower than the peak at –9 lag (Fig. 13C).

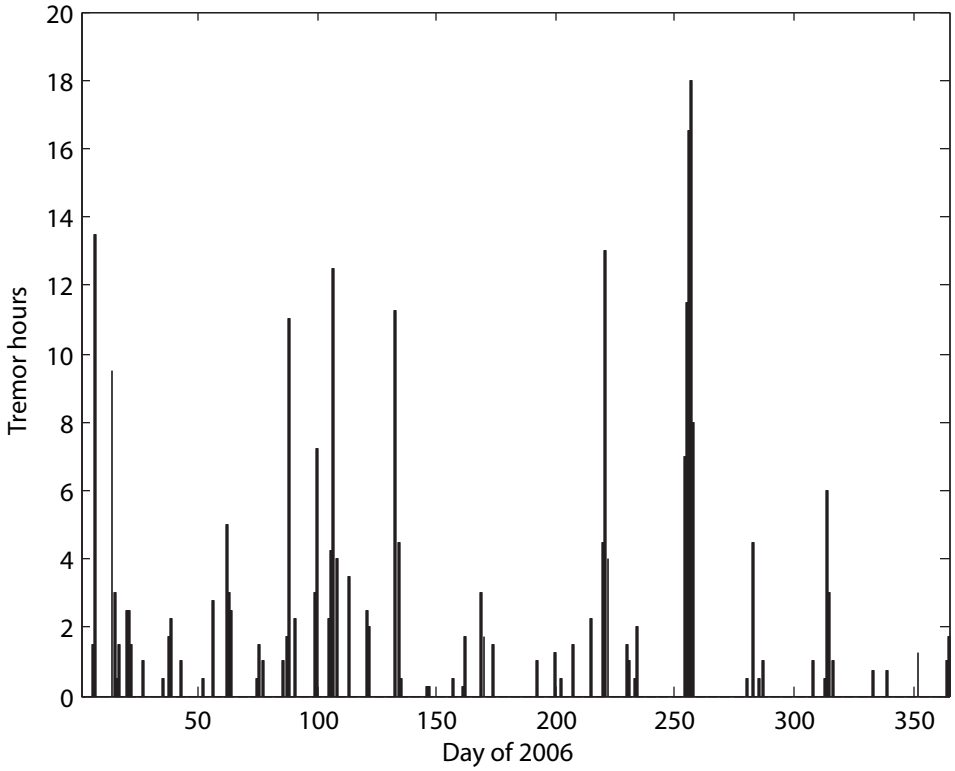

Figure 10. Hours of tremor per day for the year 2006.

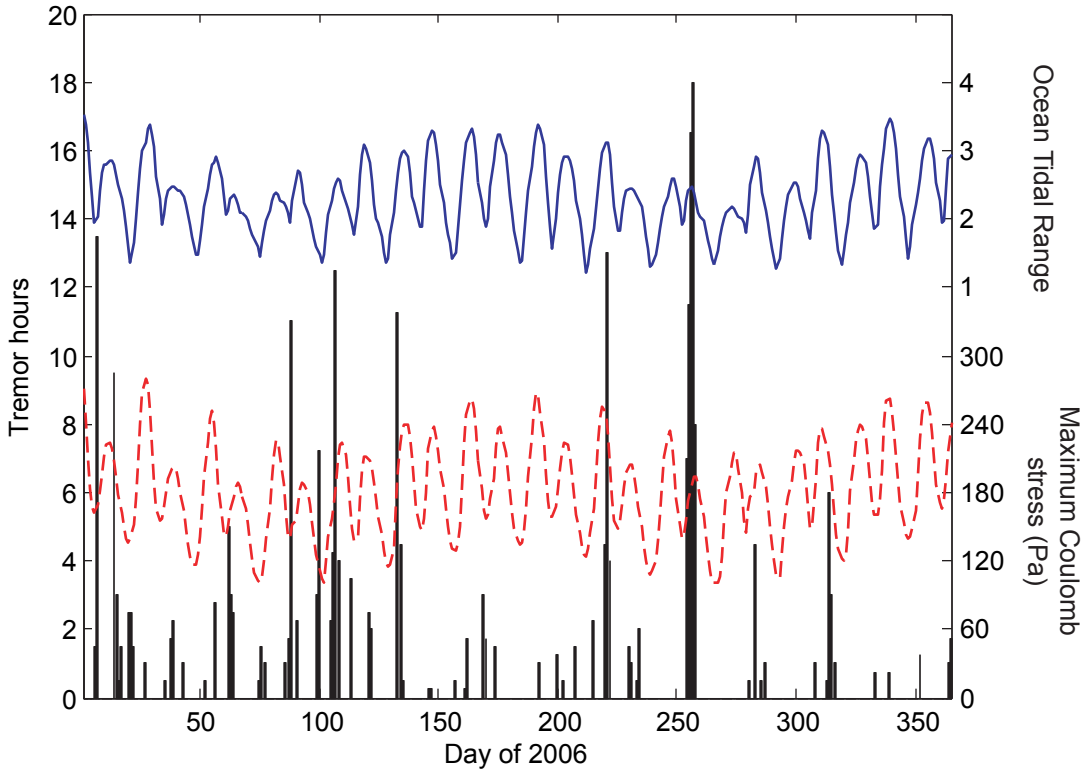

Figure 11. Tremor (black bars) plotted with ocean tidal range as measured at Sequim (solid blue line) and maximum daily Coulomb stress as measured at Hoodsport (dashed red line) for the year 2006.

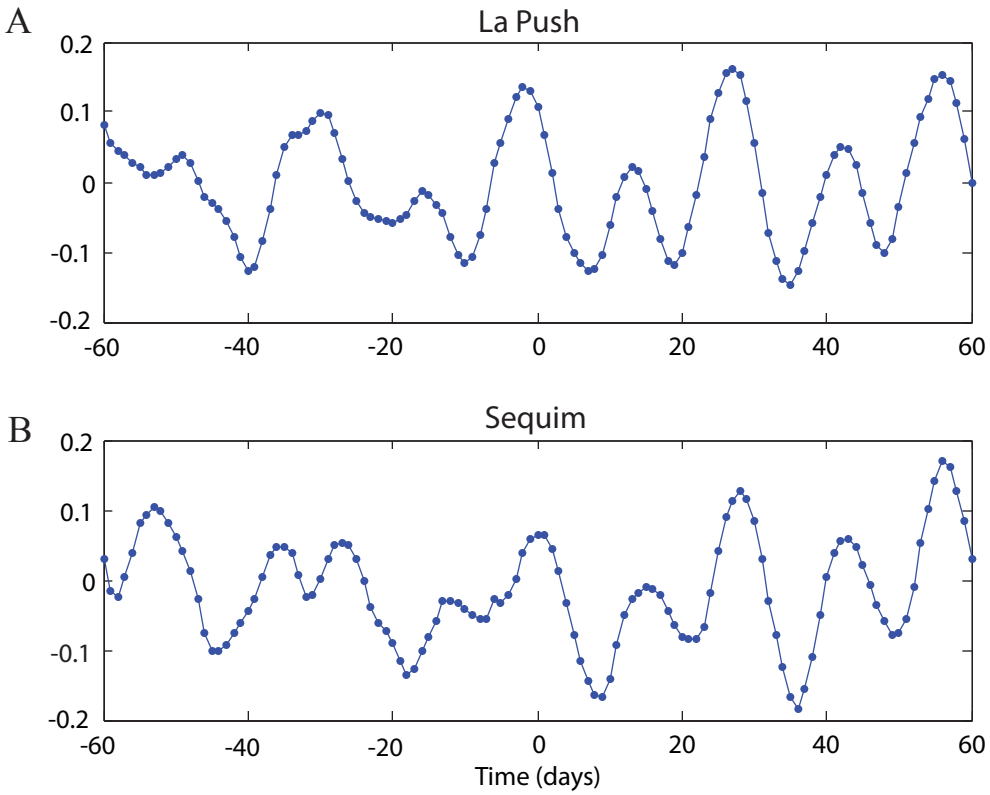

Figure 12. Cross-correlation of tremor with ocean tidal range at La Push (A) and Sequim (B), WA. The x-axis represents the number of days the time series were shifted to get the given correlation. The y-axis scale is meaningless, other than to say that the series are better correlated at higher values.

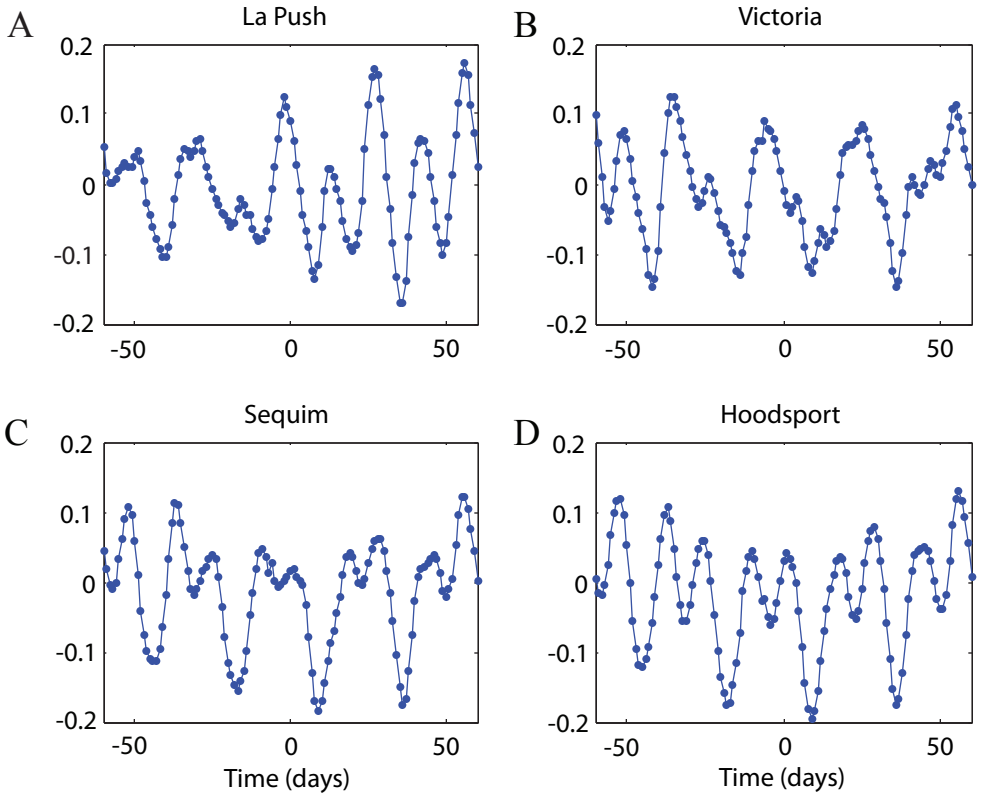

Figure 13. Cross-correlation of tremor with maximum daily Coulomb stress at La Push (A), Victoria (B), Sequim (C), and Hoodsport (D). The x-axis represents the number of days the time series were shifted to get the given correlation. The y-axis scale is meaningless, other than to say that the series are better correlated at higher values.

Figures 14A and 14B show the results of plotting the number of tremor hours and days with tremor as a function of ocean tidal range at La Push and Sequim, respectively. Both exhibit peaks in days and hours with tremor when the tidal range was near its maximum, above the amount that would be expected if tremor were distributed uniformly. As shown in Table 3, the probabilities of getting these peaks of tremor days near a maximum tidal range with a uniform distribution of tremor are 0.21 and 0.09 for the series at La Push and Sequim, respectively.

Figure 15 shows the number of tremor hours and days in relation to maximum Coulomb stress at the four sites used for this study. Similar to Figure 14, Figure 15A shows a peak near 0 with a probability of only 0.09 of being obtained with a uniform distribution of tremor. Figures 15B-D, on the other hand, do not show pronounced peaks of tremor days or hours near days with the highest Coulomb stresses, and have probabilities of 0.81, 0.40, and 0.51 of occurring with uniformly distributed tremor.

DISCUSSION

Previous Work on Correlating Earthquakes With Earth Tides

There are many previous studies that investigated correlations between earthquakes and earth tides (Emter, 1997), with positive (Wilcock, 2001), negative (McNutt and Heaton, 1981; Vidale, 1998), and mixed results (Tsuruoka et al., 1995). This study seeks to perform the same types of comparisons using tremor and Earth tides, by assuming that tremor is equivalent to slip on a fault with the same depth and geometry as the subducting Juan de Fuca plate. This is a reasonable assumption, since previous

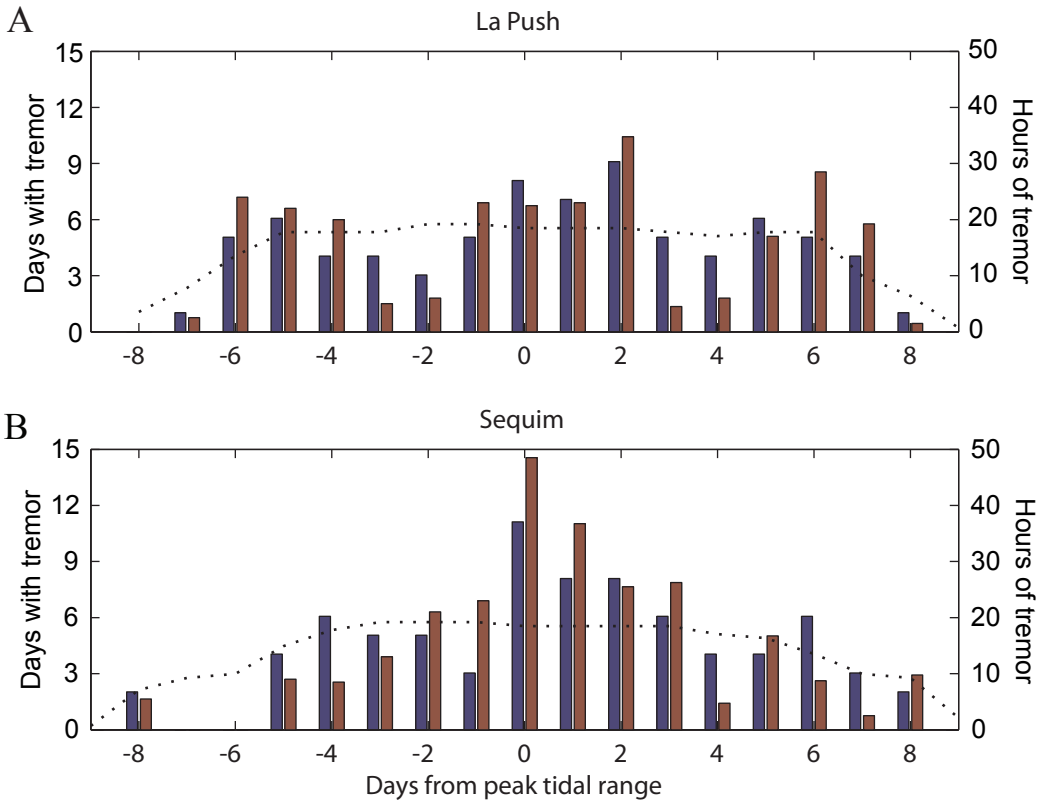

Figure 14. Histograms showing the distribution of days (blue) and hours (red) of tremor with respect to the day of a peak ocean tidal range, as recorded at La Push (A) and Sequim (B). The dotted line indicates the number of hours or days of tremor expected in a uniform tremor distribution. This line is not horizontal because the peaks of tidal ranges did not occur at regular intervals- days between peaks ranged between 9 to 17 days. Therefore, the bins on the edges did not occur as frequently.

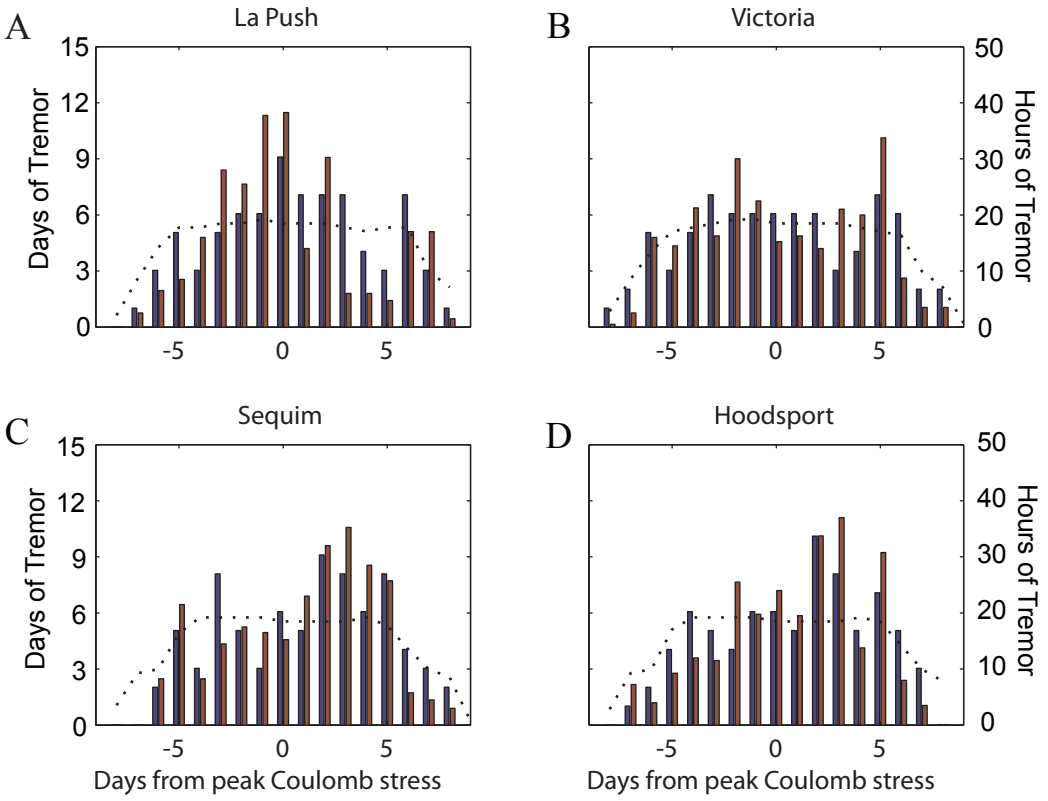

Figure 15. Histograms showing the distribution of days (blue, left bar) and hours (red, right bar) of tremor with respect to the day of a peak Coulomb stress, as recorded at La Push (A) Victoria (B), Sequim (C), and Hoodsport (D). The dotted line indicates the number of hours or days of tremor expected in a uniform tremor distribution. This line is not horizontal because the peaks of Coulomb stress did not occur at regular intervals- days between peaks ranged between 9 to 17 days. Therefore, the bins on the edges did not occur as frequently.

Table 3. Probabilities that a uniform distribution of tremor would match actual data.

	Figure number					
	14A	14B	15A	15B	15C	15D
Expected days of tremor in –1, 0, +1 bins	16.7	16.7	16.7	16.7	16.7	16.7
Probability *p* of a random day being in one of these bins	0.22	0.22	0.22	0.22	0.22	0.22
Standard deviation $\sqrt{[np(1-p)]}$, n=77	3.61	3.61	3.61	3.61	3.61	3.61
Actual days of tremor in –1, 0, +1 bins	20	22	22	14	18	17
P($X \geq$ actual) = (2)	0.21	0.09	0.09	0.81	0.40	0.51

Note: To test the significance of the peaks for tremor days, I assumed that tremor occurred randomly in 2006 and determined how likely it would be to see these distributions if that were the case. Specifically, I test the null hypothesis that tremor occurs randomly by assuming that tremor behaves like a binomially distributed random variable X. A binomial distribution is the probability distribution of the number of successes in a sequence of n Bernoulli trials, each with a probability p of succeeding. Bernoulli trials are simply trials that can either succeed or fail (in this case, tremor can occur or not occur). Since tremor occurred during 77 days in 2006, $n = 77$. The probability p of a random tremor event occurring during one of the three central bins varies between 0.22 and 0.28. In a binomial distribution, the probability that the random variable X equals a value k is equal to $P(X = k) = {}_nC_k * p^k(1- p)^{n-k}$ [${}_nC_k$ signifies 'n choose k,' which is equivalent to $n!/(k!(n-k)!)$]. Therefore, the probability that tremor occurs at least a certain number of times x is $P(X \geq x) = 1 - P(X < x) =$

$$1-\sum_{k=0}^{x-1}\binom{n}{k}p^k(1-p)^{n-k} \qquad (2)$$

work has shown that many tremor events occur at depths near the subduction interface (Rogers and Dragert, 2003; Kao et al., 2005). Studies in Japan have also shown that low-frequency earthquakes, which are closely associated with tremor, have focal mechanism solutions with nodal planes consistent with the dip of the subducting Philippine Sea plate (Shelly et al., 2006; Ito et al., 2007).

Earth tides, much like the ocean tides, are the result of the gravitational interaction between the Earth, Moon, and Sun, which deforms the solid Earth (Melchior, 1983). Average solid Earth tide stresses in the continents have amplitudes of 1-4 kPa, whereas Earth tide stresses in the oceans can reach 10 kPa, due to ocean tidal loading (Figures 6-9; Melchior, 1983; Wilcock, 2001). These values are above the average rate of tectonic stress buildup (10-100 Pa/hr or much lower- in Cascadia, where megathrust earthquakes have recurrence intervals of ~500 years [$\sim 5*10^6$ hours], the average tectonic stress can be calculated by the stress drop of a typical megathrust earthquake divided by the recurrence interval, 1-10 MPa/$5*10^6$ hours ≈ .2-2 Pa/hr), but are well below the average stress drop in earthquakes (1-10 MPa; Kanamori and Anderson, 1975). They are also well below the average lithostatic pressure in the Earth at the depths that this study focuses on. For example, the pressure on the Earth at a depth of 40 km is ~1.1 GPa, assuming a crustal density of $2.83*10^3$ kg/m^3.

Although stresses due to Earth tides are orders of magnitude smaller than stress drops from earthquakes, the fact that Earth tide stresses are greater than average rates of tectonic stress buildup suggests that earth tides can trigger tremor episodes. If average tectonic stress buildup in the Cascadia subduction zone is around 1 Pa/hour, then a modulation of this value by Earth tide stresses with amplitudes of ~1-10 kPa could cause

a critical stress amount to be reached before the average tectonic buildup reached that point (Vidale et al., 1998; Thatcher, 1982).

Discussion of the Results of this Study

The cross-correlations performed between tremor and ocean and Earth tides for this study offer interesting results (Figs 12 and 13). The strongest correlation between tremor and Earth tides occurs at La Push (Fig. 13a), most likely because of the tidal loading present at that site which creates more pronounced Coulomb stresses. Of course, La Push is not near the 40 km depth contour where most Cascadia tremor has been located, but this can be ignored by comparing the correlation between tremor and ocean tides at La Push and Sequim (which is near the 40 km depth contour)- both show correlations near zero lag, and in fact, the correlation at Sequim has a peak at 0 days (Fig. 12b) while the correlation at La Push has a peak at –2 days (Fig. 12a). Therefore, it is likely that if the Sequim tensor, for example, were taken with a large ocean tidal loading effect, it would show a correlation with tremor similar to that of La Push.

The results shown in Figures 14 and 15 are similar to the cross-correlation results. That is, the strongest evidence that tremor is related to Earth tides is found in the comparison at La Push (Fig. 15a), with a probability of only 0.09 that this distribution of tremor hours and days in relation to peak Coulomb stresses would be found with uniformly distributed tremor. The more uniformly distributed results at Victoria, Sequim, and Hoodsport could be due to the ocean tidal loading effect described above, or they could be reflecting a reality that Earth tides do not affect tremor.

The correlations and methods presented here could use some improvements (see below), but they still show a possible correlation between Earth tide stresses and tremor occurrences. If this is the case, it would indicate that tremor can be thought of as slip on a plane parallel to the Juan de Fuca plate under Washington state, and that this zone is near a critical value of stress that would allow stress fluctuations due to Earth tides to trigger a tremor episode.

Possibilities for Future Study

One problem with this study is that since the stress tensors used are calculated at the surface of the Earth, it is difficult to extrapolate stresses to depths of 30 or 40 km where tremor usually occurs. Ideally, stress tensors at these depths would be used, but there are currently no established methods for doing this (Agnew, 2006; Wilcock, 2006). It is possible that the effect of ocean tidal loading would extend inland from the ocean at these depths, or, alternatively, the Earth tides alone would dominate. However, it is likely that the stresses due to Earth tides would remain qualitatively the same (Creager, 2007), so the methods used in this study are still valid.

This study would also benefit from an extended time series of tremor. Since data was only examined for the year 2006, only 77 days with tremor were recorded. Compare this with other studies that examined correlations between Earth tides and earthquakes which used data sets containing anywhere from 988 to 13,042 earthquakes (Tsuruoka et al., 1995; Vidale et al., 1998; McNutt and Heaton, 1981; Wilcock, 2001). Larger data sets help to reduce the effects of outliers, and provide more reliable results.

Since Coulomb stresses due to tides vary daily, comparisons between tremor and Coulomb stresses should be performed on a daily scale. If the two were related, one would expect to see more tremor occurring during hours of low tide (corresponding to high Coulomb stresses) and less tremor occurring during hours of high tide (corresponding to low Coulomb stresses). Although in this study I did record the hours of tremor episodes, the resolution was not on a fine enough scale.

A better way to examine the relationship between tremor and Coulomb stresses on a daily scale would be to examine the amplitude of tremor during the 14-month episodic tremor and slip events, in which tremor is occurring almost continuously. Since the tremor amplitude would be a continuous data set, it would be simple to compare it with variations in the tidal cycle. A good data set to use would be from the most recent episodic tremor and slip event that occurred in late January and early February of 2007.

CONCLUSIONS

In this study I determined that tremor in the Cascadia subduction zone occurred during the year 2006 as a number of small events usually lasting fewer than three days. Furthermore, after comparison with Coulomb stresses due to Earth tides and ocean tidal loading, there is some enticing evidence in support of the hypothesis that tidal stresses can trigger tremor. However, one would have to perform an analysis with larger data sets and more rigorous statistical tests in order to confirm this hypothesis with certainty.

ACKNOWLEDGEMENTS

This project was started in the summer of 2006 as part of an IRIS (Incorporated Research Institutions for Seismology) internship at the University of Washington. I worked closely with my faculty advisor at the University of Washington, Ken Creager, and a graduate student, Aaron Wech. My advisor at Carleton was Sarah Titus, who was very helpful. Duncan Agnew (UCSD- Scripps Institution of Oceanography) and William Wilcock (University of Washington) provided code and advice on Earth tides and ocean tidal loading. I am very grateful to all of these people (and organization), as well as anyone else who provided help and/or support along the way.

REFERENCES CITED

Abers, G.A., Rondenay, S., Creager, K.C., Malone, S., Wech, A., Zhang, Z., Melbourne, T., Hacker, B., 2007, Imaging subduction, episodic tremor and slip in the Pacific Northwest: Cascadia arrays for earthscope (CAFE): Earthscope abstract.

Agnew, D, 1997, SPOTL: some programs for ocean-tide loading, SIO Reference Series 96-8, Scripps Institution of Oceanography.

Agnew, D., December 14, 2006, Personal communication.

Atwater, B. F., 1987, Evidence for great Holocene earthquakes along the outer coast of Washington State: Science, v. 236, no. 4804, p. 942-944.

Chiao, L., Creager, K.C., 2002, Geometry and membrane deformation rate of the subducting Cascadia slab: U.S. Geological Survey Open-File Report 02-328, 182 p.

Cocco, M., and Rice, J. R., 2002, Pore pressure and poroelasticity effects in Coulomb stress analysis of earthquake interactions: Journal of Geophysical Research-Solid Earth, v. 107, no. B2, p. 17.

Creager, K.C., March 7, 2007, Personal communication.

Crosson, R. S., and Owens, T. J., 1987, Slab geometry of the Cascadia subduction zone beneath Washington from earthquake hypocenters and teleseismic converted waves: Geophysical Research Letters, v. 14, no. 8, p. 824-827.

Demets, C., Gordon, R. G., Argus, D. F., and Stein, S., 1990, Current plate motions: Geophysical Journal International, v. 101, no. 2, p. 425-478.

Dragert, H., Wang, K. L., and James, T. S., 2001, A silent slip event on the deeper Cascadia subduction interface: Science, v. 292, no. 5521, p. 1525-1528.

Emter, D., 1997, Tidal triggering of earthquakes and volcanic events, in *Tidal Phenomena*, edited by S. Bhattacharji, G. Friedman, H.J. Neugebauer, and A. Seilacher, pp. 293-309, Springer, New York.

Geological Survey of Canada website, http://gsc.nrcan.gc.ca/geodyn/casaction_e.php, visited February 2, 2007.

Harris, R. A., 1998, Introduction to special section: Stress triggers, stress shadows, and implications for seismic hazard: Journal of Geophysical Research-Solid Earth, v. 103, no. B10, p. 24347-24358.

Hyndman, R. D., Wang, K., Dragert, H, 1997, Cascadia megathrust earthquake potential: constraints from current deformation and the thermal regime, USGS annual summary vol. 37. 1997.

Ito, Y., Obara, K., Shiomi, K., Sekine, S., and Hirose, H., 2007, Slow earthquakes coincident with episodic tremors and slow slip events: Science, v. 315, no. 5811, p. 503-506.

Johnston, M. J. S., Borcherdt, R. D., Linde, A., and Gladwin, M. T., 2006, Continuous borehole strain and pore pressure in the near field of the 28 September 2004 M 6.0 Parkfield, California, earthquake: Implications for nucleation, fault response, earthquake prediction, and tremor: Bulletin of the Seismological Society of America, v. 96, no. 4, p. S56-S72.

Kanamori, H., and Anderson, D. L., 1975, Theoretical basis of some empirical relations in seismology: Bulletin of the Seismological Society of America, v. 65, no. 5, p.

1073-1095.
Kao, H., Shan, S. J., Dragert, H., Rogers, G., Cassidy, J. F., and Ramachandran, K., 2005, A wide depth distribution of seismic tremors along the northern Cascadia margin: Nature, v. 436, no. 7052, p. 841-844.
McCausland, W., Malone, S., and Johnson, D., 2005, Temporal and spatial occurrence of deep non-volcanic tremor: From Washington to northern California: Geophysical Research Letters, v. 32, no. 24, p. 4.
McNutt, M., and Heaton, T., 1981, An evaluation of the seismic-window theory for earthquake prediction: California Geology, v. 34, no. 1, p. 12-16.
Melchior, P, 1983, The tides of planet earth, 641 pp., Pergamon, New York.
NOAA website, http://tidesonline.nos.noaa.gov/. Ocean tidal data from National Oceanic and Atmosphere Administration, accessed February 10, 2007.
Obara, K., 2002, Nonvolcanic deep tremor associated with subduction in southwest Japan: Science, v. 296, no. 5573, p. 1679-1681.
Preston, L. A., Creager, K. C., Crosson, R. S., Brocher, T. M., and Trehu, A. M., 2003, Intraslab earthquakes: Dehydration of the Cascadia slab: Science, v. 302, no. 5648, p. 1197-1200.
Rogers, G., and Dragert, H., 2003, Episodic tremor and slip on the Cascadia subduction zone: The chatter of silent slip: Science, v. 300, no. 5627, p. 1942-1943.
Satake, K., Shimazaki, K., Tsuji, Y., and Ueda, K., 1996, Time and site of a giant earthquake in Cascadia inferred from Japanese tsunami records of January 1700: Nature, v. 379, no. 6562, p. 246-249.
Schwiderski, E. W., 1980, On charting global ocean tides: Reviews of Geophysics, v. 18, no. 1, p. 243-268.
Shelly, D. R., Beroza, G. C., Ide, S., and Nakamula, S., 2006, Low-frequency earthquakes in Shikoku, Japan, and their relationship to episodic tremor and slip: Nature, v. 442, no. 7099, p. 188-191.
Thatcher, W., 1982, Seismic triggering and earthquake prediction: Nature, v. 299, no. 5878, p. 12-13.
Trehu, A.M., Brocher, T.M., Creager, K.C., Fisher, M.A., Preston, L.A., Spence, G., and the SHIPS98 Working Group, 2002, Geometry of the subducting Juan de Fuca plate: New constraints from SHIPS98: U.S. Geological Survey Open-File Report 02-328, 182 p.
Tsuruoka, H., Ohtake, M., and Sato, H., 1995, Statistical test of the tidal triggering of earthquakes: contribution of the ocean tide loading effect: Geophysical Journal International, v. 122, no. 1, p. 183-194.
Vidale, J. E., Agnew, D. C., Johnston, M. J. S., and Oppenheimer, D. H., 1998, Absence of earthquake correlation with Earth tides: An indication of high preseismic fault stress rate: Journal of Geophysical Research-Solid Earth, v. 103, no. B10, p. 24567-24572.
Wells, R.E., Blakely, R.J., Weaver, C.S., 2002, Cascadia microplate model and within-slab earthquakes: U.S. Geological Survey Open-File Report 02-328, 182 p.
Wilcock, W. S. D., 2001, Tidal triggering of micro earthquakes on the Juan de Fuca Ridge: Geophysical Research Letters, v. 28, no. 20, p. 3999-4002.
Wilcock, W., December 6, 2006, Personal communication.
Wilson, D.S., 2002, The Juan de Fuca plate and slab: Isochron structure and Cenozoic

plate motions: U.S. Geological Survey Open-File Report 02-328, 182 p.
Wilson, D. S., 1988, Tectonic history of the Juan de Fuca ridge over the last 40 million years: Journal of Geophysical Research-Solid Earth and Planets, v. 93, no. B10, p. 11863-11876.

Appendix A: Stress tensor calculations

Plane defined by three vectors:
v_1 (strike) = <cos *a*, sin *a*, 0>;
v_2 (dip) = <-sin *a* cos *b*, cos *a* cos *b*, sin *b*>;
v_3 (normal) = <sin *a* sin *b*, -cos *a* sin *b*, cos *b*>;
v_{slip} (in direction of plate motion) = slip-dot(slip,v_3)*v_3, where slip=<cos(*dir*) sin(*dir*) 0>;

a = angle of strike, and *b* = angle of dip, *dir* = plate motion direction

$T=dot(\sigma,v_3)$ -Where T=traction vector, σ=stress tensor and dot() means dot product;
$|\sigma_n|=dot(T,v_3)$ -(normal stress) [| | means magnitude];
$|\sigma_s|=dot(T,v_{slip})$ -(shear stress);

Check if: $|\sigma_s| > \mu(-|\sigma_n|-Pf)$ where μ is the coefficient of friction (usually from .5-1) and Pf is pore pressure;

Appendix B: Tremor events for 2006

Event	Starting date	Number of days in event	Hours/day	Event	Starting date	Number of days in event	Hours/day
1	1/6/2006	2	1.5	19	6/6/2006	1	0.5
			13.5	20	6/10/2006	2	0.25
2	1/14/2006	4	9.5				1.75
			3	21	6/18/2006	2	3
			0.5				1.75
			1.5	22	6/23/2006	1	1.5
3	1/20/2006	3	2.5	23	7/11/2006	1	1
			2.5	24	7/19/2006	3	1.25
			1.5				0
4	1/27/2006	1	1				0.5
5	2/4/2006	1	0.5	25	7/26/2006	1	1.5
6	2/7/2006	2	1.75	26	8/3/2006	1	2.25
			2.25	27	8/8/2006	3	4.5
7	2/12/2006	1	1				13
8	2/21/2006	1	0.5				4
	2/25/2006	1	2.75	28	8/18/2006	2	1.5
9	3/3/2006	3	5				1
			3	29	8/21/2006	2	0.5
			2.5				2
10	3/16/2006	3	0.5	30	9/11/2006	5	7
			1.5				11.5
			1				16.5
11	3/27/2006	3	1				18
			1.75				8
			11	31	10/7/2006	1	0.5
12	4/1/2006	1	2.25	32	10/10/2006	5	4.5
13	4/9/2006	2	3				0
			7.25				0.5
14	4/15/2006	4	2.25				0
			4.25				1
			12.5	33	11/4/2006	1	1
			4	34	11/9/2006	4	0.5
15	4/23/2006	1	3.5				6
16	5/1/2006	2	2.5				3
			2				1
17	5/13/2006	3	11.25	35	11/29/2006	1	0.75
			4.5	36	12/5/2006	1	0.75
			0.5	37	12/18/2006	1	1.25
18	5/26/2006	2	0.25	38	12/30/2006	2	1
			0.25				1.75

Appendix C: Matlab code

Figures2.m- Assemble all data and make figures

```
%Assemble all data and make figures

load tremor2006.txt;
load tides2006a.txt;
load tides2006b.txt;
load tensor2006a.txt;
%load tensor2006a2.txt;
load tensor2006b.txt;
load tensor2006c.txt;
load tensor2006d.txt;

tremor=tremor2006;
tidesa=tides2006a;
tidesb=tides2006b;
tensa=tensor2006a;
%tensa2=tensor2006a2;
tensb=tensor2006b;
tensc=tensor2006c;
tensd=tensor2006d;

[sheara,normala,failuresa,maxfailurea]=tremtenstide5(tensa,315,11);
%[sheara2,normala2,failuresa2,maxfailurea2]=tremtenstide5(tensa2,315,11
);
[shearb,normalb,failuresb,maxfailureb]=tremtenstide5(tensb,345,11);
[shearc,normalc,failuresc,maxfailurec]=tremtenstide5(tensc,315,11);
[sheard,normald,failuresd,maxfailured]=tremtenstide5(tensd,0,11);

tbig=[1:1/48:365.99];
intday=[1:365];

for i=1:365;
  i1=find(abs(intday(i)+.5-tbig)<14/24);%gets indices of tbig
corresponding
                                        %to integer days with 2 hours
of
                                        %space on either side to
account
                                        %for tidal phase shift
  rangea(i)=max(tidesa(i1))-min(tidesa(i1));
  rangeb(i)=max(tidesb(i1))-min(tidesb(i1));
  i2=find(abs(intday(i)+.5-tbig)<.5);   %gets indices of tbig
corresponding
                                        %to integer days
  mintidea(i)=min(tidesa(i2));
  mintideb(i)=min(tidesb(i2));
end

%determine number of tremor hours/days within bins around maximum tides
[daysA,tremhA,tremdA,testA]=rangetest5(maxfailurea);
[daysB,tremhB,tremdB,testB]=rangetest5(maxfailureb);
[daysC,tremhC,tremdC,testC]=rangetest5(maxfailurec);
```

```
[daysD,tremhD,tremdD,testD]=rangetest5(maxfailured);
[daysAt,tremhAt,tremdAt,testAt]=rangetest5(rangea);
[daysBt,tremhBt,tremdBt,testBt]=rangetest5(rangeb);

%perform crosscorrelations of tremor and tidal series
[Xat,LAGSat]=montecorr(tremor,rangea);
[Xbt,LAGSbt]=montecorr(tremor,rangeb);
[Xa,LAGSa]=montecorr(tremor,maxfailurea);
[Xb,LAGSb]=montecorr(tremor,maxfailureb);
[Xc,LAGSc]=montecorr(tremor,maxfailurec);
[Xd,LAGSd]=montecorr(tremor,maxfailured);

%plot cross-correlations
figure(41);%tremor and ocean tidal range
subplot(2,1,1);
plot(LAGSat,Xat,'.-');

subplot(2,1,2);
plot(LAGSbt,Xbt,'.-');

figure(42);
subplot(2,2,1);%La Push
plot(LAGSa,Xa,'.-');

subplot(2,2,2);%Victoria
plot(LAGSc,Xc,'.-');

subplot(2,2,3);%Sequim
plot(LAGSb,Xb,'.-');

subplot(2,2,4);%Hoodsport
plot(LAGSd,Xd,'.-');

t1=14593;%Nov. 1 (day 305)
t2=14641;%Nov. 2 (day 306)
t3=16033;%Dec. 1 (day 335)

%plot number of tremor hours/days in bins around tidal maxima
clear abox;
clear bbox;
clear cbox;
clear dbox;

dhscale=3.37;%to get days and hours on the same scale
scaled=.211;%77/365, likelihood of tremor/day

%Tremor and ocean tides
figure(31);clf;
subplot(2,1,1);
abox(1,:)=tremdAt*dhscale;abox(2,:)=tremhAt;
bar(daysAt,abox','grouped');hold on;
plot(daysAt,testAt*scaled*dhscale,'k:');
axis([-9 9 0 50]);
ylabel('Tremor hours [r] (day*4 [b])');
title('La Push');
```

```
subplot(2,1,2);
bbox(1,:)=tremdBt*dhscale;bbox(2,:)=tremhBt;
bar(daysBt,bbox','grouped');hold on;
plot(daysBt,testBt*scaled*dhscale,'k:');
axis([-9 9 0 50]);
ylabel('Tremor hours [r] (day*4 [b])');
title('Sequim');
xlabel('Days from peak tidal range');

%Tremor and Coulomb stresses
clear abox;
clear bbox;
clear cbox;
clear dbox;
figure(32);clf;
subplot(2,2,1);%La Push
abox(1,:)=tremdA*dhscale;abox(2,:)=tremhA;
bar(daysA,abox','grouped');hold on;
plot(daysA,testA*scaled*dhscale,'k:');
axis([-9 9 0 50]);
ylabel('Tremor hours [r] (day*4 [b])');
title('La Push');

subplot(2,2,2);%Victoria
cbox(1,:)=tremdC*dhscale;cbox(2,:)=tremhC;
bar(daysC,cbox','grouped');hold on;
plot(daysC,testC*scaled*dhscale,'k:');
axis([-9 9 0 50]);
title('Victoria');

subplot(2,2,3);%Sequim
bbox(1,:)=tremdB*dhscale;bbox(2,:)=tremhB;
bar(daysB,bbox','grouped');hold on;
plot(daysB,testB*scaled*dhscale,'k:');
axis([-9 9 0 50]);
ylabel('Tremor hours [r] (day*4 [b])');
title('Sequim');
xlabel('Days from peak Coulomb stress');

subplot(2,2,4);
dbox(1,:)=tremdD*dhscale;dbox(2,:)=tremhD;
bar(daysD,dbox','grouped');hold on;
plot(daysD,testD*scaled*dhscale,'k:');
axis([-9 9 0 50]);
title('Hoodsport');
xlabel('Days from peak Coulomb stress');

%Tides vs. stresses at La Push on Nov. 1(stresses in the ocean)
figure(12);clf;
subplot(2,1,1);plot(tbig(t1:t2),tidesa(t1:t2),'b');
axis([305 306 -1 1]);
ylabel('Tide height (m)');
title('Tide height at La Push, Nov. 1');
subplot(2,1,2);plot(tbig(t1:t2),sheara(t1:t2),'r');hold on;
plot(tbig(t1:t2),normala(t1:t2),'g--');
```

```
plot(tbig(t1:t2),failuresa(t1:t2),'k-.');
axis([305 306 -10^4 10^4]);
ylabel('Stress (Pa)');
title('Shear, normal, and max Coulomb at La Push');
xlabel('Day of 2006');

%Tides vs. stresses at Sequim on Nov. 1(stresses on land)
figure(13);clf;
subplot(2,1,1);plot(tbig(t1:t2),tidesb(t1:t2),'b');
%axis([305 306 -1 1]);
ylabel('Tide height (m)');
title('Tide height at Sequim, Nov. 1');
subplot(2,1,2);plot(tbig(t1:t2),shearc(t1:t2),'r');hold on;
plot(tbig(t1:t2),normalc(t1:t2),'g--');
plot(tbig(t1:t2),failuresc(t1:t2),'k-.');
%axis([305 306 -300 300]);
ylabel('Stress (Pa)');
title('Shear, normal, and max Coulomb at Sequim');
xlabel('Day of 2006');

%Tides vs. stresses at La Push for November (stresses in the ocean)
figure(13);clf;
subplot(2,1,1);plot(tbig(t1:t3),tidesa(t1:t3),'b');
axis([305 335 -2 2]);
ylabel('Tide height (m)');
title('Tide height at La Push for November');
subplot(2,1,2);plot(tbig(t1:t3),sheara(t1:t3),'r');hold on;
plot(tbig(t1:t3),normala(t1:t3),'g:');
plot(tbig(t1:t3),failuresa(t1:t3),'k-.');
axis([305 335 -2*10^4 2*10^4]);
ylabel('Stress (Pa)');
title('Shear, normal, and max Coulomb at La Push');
xlabel('Day of 2006');

%Tides vs. stresses at Sequim for November (stresses in the ocean)
figure(14);clf;
subplot(2,1,1);plot(tbig(t1:t3),tidesb(t1:t3),'b');
axis([305 335 -2 2]);
ylabel('Tide height (m)');
title('Tide height at Sequim for November');
subplot(2,1,2);plot(tbig(t1:t3),shearb(t1:t3),'r');hold on;
plot(tbig(t1:t3),normalb(t1:t3),'g:');
plot(tbig(t1:t3),failuresb(t1:t3),'k-.');
axis([305 335 -700 700]);
ylabel('Stress (Pa)');
title('Shear, normal, and max Coulomb at Sequim');
xlabel('Day of 2006');

%Plot tremor
figure(21);%tremor
bar(tremor,'k');
axis([1 365 0 20]);
title('Tremor during 2006');
xlabel('Day of 2006');
ylabel('Tremor hours');
```

```
%Plot tremor with both tide series
figure(22);clf%tremor with tidal range and Coulomb stress
bar(intday,tremor,'k');hold on;
plot(intday,rangeb*2+8,'b');
plot(intday,maxfailured/30,'r--');
axis([1 365 0 20]);
title('Tremor, tidal range (sequim) and max Coulomb stress
(hoodsport)');
xlabel('Day of 2006');
ylabel('Tremor hours');
```

tremtenstide5.m- Calculates Coulomb stresses at given point

```
function
[sheardir,normal,failures,maxfailure]=tremtenstide4(tensor,strike,dip);
%Determine Coulomb stresses at given location

a=strike;  %slab strike
b=dip;   %slab dip
mu=.6;  %coefficient of friction (unitless?)
Pf=0; %pore pressure (MPa)
dir=55; %slab movement direction (from N)

%Slab geometry vectors
v1=[cosd(a), sind(a), 0];                          %strike
v2=[-sind(a)*cosd(b), cosd(a)*cosd(b), sind(b)];%dip
v3=[sind(a)*sind(b), -cosd(a)*sind(b), cosd(b)];%normal
slip=[cosd(dir) sind(dir) 0];%direction of plate motion at surface
vslip=slip-dot(slip,v3)*v3;  %projection onto plane
vslip=vslip/sqrt(dot(vslip,vslip));%unit vectored

%Compute failure amount for each point
failures=[1:length(tensor)];
for i=1:length(tensor);
  row=i;%testing
  S= [tensor(row,1), tensor(row,6), tensor(row,5);
      tensor(row,6), tensor(row,2), tensor(row,4);
      tensor(row,5), tensor(row,4), tensor(row,3);];

  t2 = S*v3';
  ns2=v3*t2;
  ss2=v2*t2;
  ss3=vslip*t2;

  shear(i)=ss2;
  sheardir(i)=ss3;%ss in plate motion direction
  normal(i)=ns2;

  x=ss3+mu*ns2;
  failures(i)=x;
end;

maxfailure=[1:365];
for iday=1:365;
  maxf=failures((iday-1)*48+1);
```

```
  for ihour=1:48;
    index=(iday-1)*48+ihour;
    if failures(index)>maxf;
        maxf=failures(index);
    end;
  end;
  maxfailure(iday)=maxf;
end
```

rangetest5.m- put tremor hours/days in bins around tidal maxima

```
function [days,tremh,tremd,test] = rangetest4(series);
%takes a peak series and determines the amount of tremor in the days
around
%them

%load tensor2006d.txt;
%tensd=tensor2006d;
%[sheard,normald,failuresd,maxfailured]=tremtenstide5(tensd,0,11);
%series=maxfailured;

load tremor2006.txt;
tremor=tremor2006;

tbig=[1:1/48:365.99];
intday=[1:365];

A=diff(series);
ind=find(A(1:363)>0 & A(2:364)<0);
ind(length(ind)+1)=ind(length(ind))+14;
%for i=1:length(ind);
%    peaks(ind(i)+1)=1;
%end
peaks=ind+1;

maxNum=max(diff(ind));

index=0;
for j=1:maxNum;
  tremh(j)=0;
  tremd(j)=0;
  test(j)=0;
end

%go through year, put tremor hours into day boxes
for i=1:365;
  if i>=peaks(index+1);%keep the window between two syzygys
    index=index+1;
  end

  if index==0;
    d1=-i;
  else
    d1=peaks(index)-i;
```

```
  end
  d2=peaks(index+1)-i;

  if abs(d1)<d2;
    d=d1;
  else
    d=d2;
  end

  mid=ceil(maxNum/2);
  tremh(mid+d)=tremh(mid+d)+tremor(i);
  if tremor(i)~=0;
    tremd(mid+d)=tremd(mid+d)+1;
  end
  test(mid+d)=test(mid+d)+1;
end

days=-floor(maxNum/2):floor(maxNum/2);
if (length(days)>length(tremd));
    days=days(2:length(days));
end
```

montecorr.m- Returns a cross-correlation of two data sets using the matlab command xcorr (different version than xcor)

```
function [X,LAGS] = montecorr(totaltrem,range);
%takes a tremor daily series and tide range daily series and xcorr's
the s* out of them

intday=[1:365];
time_clip=5;
g=range-mean(range);
f=totaltrem-mean(totaltrem);
%f = totaltrem; f=min(f,time_clip); f=f-mean(f);
[X,LAGS]=xcorr(g,f,60,'coeff');
```